Poly(fluorenevinylene) Copolymers Containing Bis(phenyl)oxadiazole and Triphenylamine Moieties: Synthesis, Photophysics, and Redox and Electroluminescent Properties

John A. Mikroyannidis,*,† Katherine M. Gibbons,‡ Abhishek P. Kulkarni,‡ and Samson A. Jenekhe*,‡

Chemical Technology Laboratory, Department of Chemistry, University of Patras, GR-26500 Patras, Greece, and Departments of Chemical Engineering and of Chemistry, University of Washington, Seattle, Washington 98195

Received July 8, 2007; Revised Manuscript Received November 10, 2007

ABSTRACT: New fluorescent fluorenevinylene copolymers incorporating bis(phenyl)oxadiazole, triphenylamine, or both moieties were synthesized, characterized, and used as the emissive materials in efficient electroluminescent diodes. In dilute solutions, the copolymers had blue-green fluorescence with high quantum yields of 0.76−0.87. All the copolymers had high glass transition temperatures (T_g = 147−160 °C) and outstanding thermal stability. Light emitting diodes based on the neat copolymer thin films showed bright greenish-yellow electroluminescence, with luminances of up to 1360 cd/m^2, originating mostly from intramolecular charge-transfer excited states due to the presence of the donor/acceptor moieties in the copolymers. However, dilute (approximately 5 wt %) binary blends of the copolymers with poly(vinyl carbazole) gave stable blue electroluminescence (CIE = 0.17, 0.16) with higher luminances (1770−3400 cd/m^2) and luminous efficiencies of up to 1.34 cd/A.

Introduction

Conjugated polymer based light-emitting diodes (PLEDs) have attracted considerable interest because of their applications in flat-panel displays.[1] Among the classes of electroluminescent (EL) conjugated polymers, two have attracted the most general interest: poly(*p*-phenylenevinylene)s (PPVs) and poly(9,9-dialkylfluorene)s (PFs). Soluble EL polymer semiconductors, such as poly[(2-ethylhexyloxy-5-methoxy-1,4-phenylene)vinylene] (MEH−PPV), opened up the possibility of making PLEDs by simple solution processing techniques.[2] Similarly, PFs have been demonstrated as effective blue emitters for PLEDs.[1,3−6] However, these types of polyfluorenes usually exhibit a red-shifted green emission during device fabrication and operation. The green emission band in EL spectra has been attributed to aggregates and/or excimers.[4] An alternative explanation for the green emission band is that it is caused by keto defects arising from oxidation at the C9 positions of fluorene units that have not been fully alkylated.[5]

Another drawback for PFs in PLED applications is their high ionization potential (IP = 5.8 eV),[6] resulting in a high-energy barrier for injection of holes into the PFs from the indium tin oxide (ITO)/poly(3,4-ethylenedioxythiophene) (PEDOT) layer (work function = 5.2 eV) commonly used as the anode in PLEDs.[7] Higher driving voltages also result from the large IP of PFs.[8] Although blends prepared by doping PFs with hole-transporting molecules have led to some improvement in hole injection from the PEDOT anode, as well as EL device stability;[9] physical blending of small molecules into a polymeric host runs the risk of phase separation over time. The incorporation of electron-rich tertiary aromatic amines into polyfluorene backbones can lead to copolymers having much lower IP values (5.0−5.3 eV)[10] that are better matched with the work function of the ITO/PEDOT layer (5.2 eV). Consequently, devices based on these copolymers exhibit lower operating voltages relative to those of devices based on the corresponding fluorene homopolymers.[11]

Recently, poly(9,9-dialkylfluorene-2,7-vinylene)s were prepared by acyclic diene metathesis (ADMET) polymerization,[12] Heck[13] or Wittig[13,14] reaction, Gilch polymerization,[15] and Suzuki coupling.[13,16] Moreover, 2,7-fluorenevinylene based trimer-model compounds were very recently synthesized and used as emissive materials in LEDs.[17] EL polymers containing both electron- and hole-transporting segments as well as emissive groups have been synthesized as a means to balance the transport of electrons and holes.[1e,18−20] 2,5-Diaryl-1,3,4-oxadiazole molecules and related derivatives are electron-deficient materials that possess good thermal and chemical stabilities as well as high photoluminescence quantum yields,[21,22] leading to their common use as electron-transport materials in LEDs.[22,23] Because triphenylamine has good hole-transporting and solubility properties,[24] several research groups have introduced oxadiazole and triphenylamine units into a polymer backbone or as the side groups to adjust the charge injection/transport properties in PLEDs.[1e,19a,20c,25]

In this paper, we describe the synthesis, characterization, photophysics, and the redox and EL properties of a series of three new conjugated poly(fluorenevinylene)s incorporating oxadiazole, triphenylamine, or both moieties along the backbone. They were synthesized by Heck coupling and contained solubilizing *n*-hexyl groups at the C-9 of fluorene. These copolymers whose molecular structures are shown in Chart 1, include: poly(fluorenevinylene-*alt*-diphenyloxadiazole) (PFV−OXD), poly(fluorenevinylene-*alt*-triphenylamine) (PFV-TPA), and statistical poly(fluorenevinylene-*co*-diphenyloxadiazole-*co*-triphenylamine) (PFV−COP). In these copolymers, the electron and/or hole transporting segments were directly incorporated into the backbone and not as pendant groups. Such an incorporation of donor/acceptor segments along the conjugated copolymer backbone is expected to directly influence the

* To whom correspondence should be addressed. E-mail: mikroyan@chemistry.upatras.gr (J.A.M.) or jenekhe@u.washington.edu (S.A.J.).

† Chemical Technology Laboratory, Department of Chemistry, University of Patras

‡ Departments of Chemical Engineering and Chemistry, University of Washington.

10.1021/ma071504l CCC: $40.75
Published on Web 12/29/2007

Chart 1

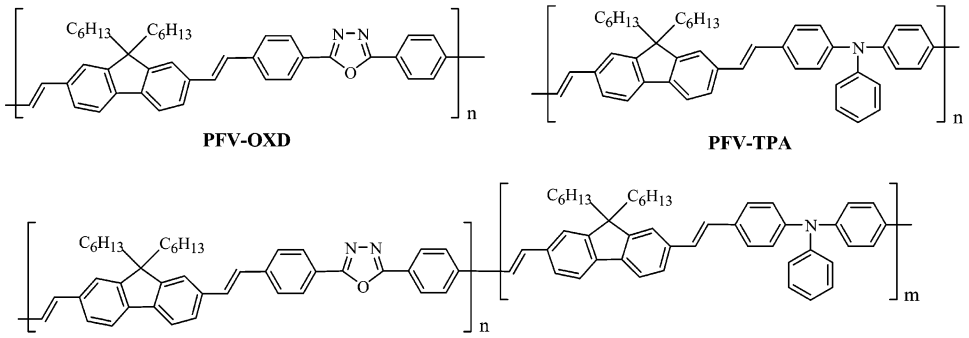

PFV-OXD **PFV-TPA**

PFV-COP n : m = 1 : 1

electron and hole delocalizations and thus carrier transport and recombination in PLEDs.

Experimental Section

Reagents and Solvents. 2,7-Dibromofluorene was synthesized according to a reported procedure.[26] 2,7-Dibromo-9,9-dihexylfluorene was synthesized by the reaction of 2,7-dibromofluorene with 1-bromohexane, catalyzed by concentrated NaOH (aqueous 50% w/w) in the presence of a phase transfer catalyst, trimethylbenzylammonium chloride.[27] Dimethylformamide (DMF) was dried by distillation over CaH_2. Triethylamine was purified by distillation over KOH. All other reagents and solvents were commercially purchased and were used as supplied.

Preparation of Monomers. 9,9-Dihexyl-2,7-divinylfluorene (1). The Stille coupling reaction[28] was used to prepare compound **1**. In particular, this compound was prepared by reacting 2,7-dibromo-9,9-dihexylfluorene with tributylvinyltin in the presence of the catalyst $PdCl_2(PPh_3)_2$ plus a few crystals of 2,6-di-*tert*-butylphenol, using toluene as the solvent. The detailed synthesis and characterization of compound **1** was reported previously.[13b]

2,5-Bis(4-bromophenyl)-1,3,4-oxadiazole (2). A flask was charged with a mixture of 4-bromobenzonitrile (4.00 g, 21.9 mmol), NH_4Cl (18.80 g, 350.4 mmol), NaN_3 (22.85 g, 350.4 mmol), and DMF (80 mL). The mixture was refluxed for 3 days. It was subsequently cooled to room temperature and poured into dilute hydrochloric acid solution. The precipitate was filtered and washed thoroughly with water. The crude product was recrystallized from ethanol to afford 4-bromophenyltetrazole (1.52 g, yield 31%, mp 255−257 °C (decomposition)). A mixture of 4-bromophenyltetrazole (1.15 g, 5.11 mmol), 4-bromobenzoyl chloride (1.76 g, 8.07 mmol), and pyridine (15 mL) was refluxed for 3 days under N_2 atmosphere. The solution was poured into water, and the solid was filtered, washed with dilute hydrochloric acid, then with water, and dried. The crude product was recrystallized from dioxane (1.12 g, yield 58%, mp 257−258 °C). The spectroscopic characterization of the product was in agreement with reported literature.[29]

Bis(4-bromophenyl)phenylamine (3). This compound was prepared according to a reported method.[30]

Preparation of Copolymers. PFV−OXD. The preparation of PFV−OXD is given as a typical example for preparation of copolymers. A flask was charged with a mixture of **1** (0.3279 g, 0.848 mmol), **2** (0.3223 g, 0.848 mmol), $Pd(OAc)_2$(0.0079 g, 0.035 mmol), P(*o*-tolyl)$_3$ (0.0594 g, 0.195 mmol), DMF (6 mL), and triethylamine (2 mL). The flask was degassed and purged with N_2. The mixture was heated at 90 °C for 24 h under N_2. Then, it was filtered and the filtrate was poured into methanol. The yellow precipitate was filtered and washed with methanol. The crude product was purified by dissolving in THF and precipitating into methanol (0.29 g, 57%). FT-IR (KBr, cm^{-1}): 3024, 2952, 2926, 2854, 1606, 1546, 1492, 1466, 1418, 1182, 1068, 1014, 962, 828, 740, 710. ^{1}H NMR ($CDCl_3$, ppm): 8.16 (m, 4H, aromatic ortho to oxadiazole ring); 8.15 (m, 2H, H4 of fluorene); 7.72 (m, 4H, H1 and H3 of fluorene); 7.56−7.53 (m, 4H, aromatic meta to oxadiazole ring); 7.34, 7.25 (m, 4H, olefinic); 2.05 (m, 4H, CH_3-$(CH_2)_4CH_2$); 1.08 (m, 16H, $CH_3(CH_2)_4CH_2$); 0.77 (t, 6H, $CH_3(CH_2)_4$-CH_2). Anal. Calcd for $(C_{43}H_{44}N_2O)_n$: C, 85.39; H, 7.33; N, 4.63. Found: C, 84.75; H, 7.64; N, 4.47.

Copolymer PFV−TPA. Copolymer PFV−TPA was similarly prepared in 49% yield from the reaction of **1** with **3** in a molar ratio 1:1. FT-IR (KBr, cm^{-1}): 3026, 2926, 2854, 1592, 1506, 1492, 1464, 1322, 1278, 1102, 960, 820, 752, 694, 670, 456. ^{1}H NMR ($CDCl_3$, ppm): 7.23−7.12 (m, 19H, aromatic and 4H, olefinic); 1.99 (m, 4H, $CH_3(CH_2)_4CH_2$); 1.06 (m, 16H, $CH_3(CH_2)_4CH_2$); 0.75 (t, 6H, $CH_3(CH_2)_4CH_2$). Anal. Calcd for $(C_{47}H_{49}N)_n$: C, 89.90; H, 7.86; N, 2.23. Found: C, 89.15; H, 7.67; N, 2.19.

Copolymer PFV−COP. Copolymer PFV−COP was similarly prepared in 48% yield from the reaction of **1** with **2** and **3** in a molar ratio 2:1:1. FT-IR (KBr, cm^{-1}): 3030, 2924, 2854, 1594, 1490, 1466, 1420, 1318, 1280, 1180, 1068, 960, 822, 746, 696, 518, 452. ^{1}H NMR ($CDCl_3$, ppm): 8.17 (m, 4H, aromatic ortho to oxadiazole ring); 7.71−7.12 (m, 29H, other aromatic and 8H, olefinic); 2.03 (m, 8H, $CH_3(CH_2)_4CH_2$); 1.07 (m, 32H, $CH_3(CH_2)_4$-CH_2); 0.76 (t, 12H, $CH_3(CH_2)_4CH_2$). Anal. Calcd for $(C_{90}H_{93}N_3O)_n$: C, 87.69; H, 7.60; N, 3.41. Found: C, 86.94; H, 7.62; N, 3.45.

Characterization Methods. IR spectra were recorded on a Perkin-Elmer 16PC FT-IR spectrometer with KBr pellets. ^{1}H NMR (400 MHz) spectra were obtained using a Bruker spectrometer. Chemical shifts (δ values) are given in parts per million with tetramethylsilane as an internal standard. TGA was performed on a DuPont 990 thermal analyzer system. Ground samples of about 10 mg each were examined by thermogravimetric analysis (TGA) and the weight loss comparisons were made between comparable specimens. Dynamic TGA measurements were made at a heating rate of 20 °C/min in N_2 at a flow rate of 60 cm^3/min. Thermomechanical analysis (TMA) was performed on a DuPont 943 TMA using a loaded penetration probe at a scan rate of 10 °C/min in N_2 with a flow rate of 60 cm^3/min. The TMA experiments were conducted at least twice to ensure the accuracy of the results. The TMA specimens were pellets of 10 mm diameter and ∼1 mm thickness prepared by pressing a powder of the copolymer for 3 min under 8 kp/cm^2 at ambient temperature. The T_g is assigned by the first inflection point in the TMA curve, and it was obtained from the onset temperature of this transition during the second heating. Elemental analyses were carried out with a Carlo Erba model EA1108 analyzer.

UV−vis absorption spectra were recorded on a Perkin-Elmer model Lambda 900 UV−vis/near-IR spectrophotometer. The photoluminescence (PL) emission spectra were obtained with a Photon Technology International (PTI) Inc. model QM-2001−4 spectrofluorimeter. To measure the PL quantum yields (Φ_f), polymer solutions in spectral grade toluene were prepared. The concentration (∼10^{-5} M) was adjusted so that the absorbance of the solution would be lower than 0.1. A 10^{-5} M solution of perylene in toluene ($\Phi_f = 0.94$) was used as a standard.[31] All solutions were purged with nitrogen for 15−20 min before spectral acquisition.

Scheme 1

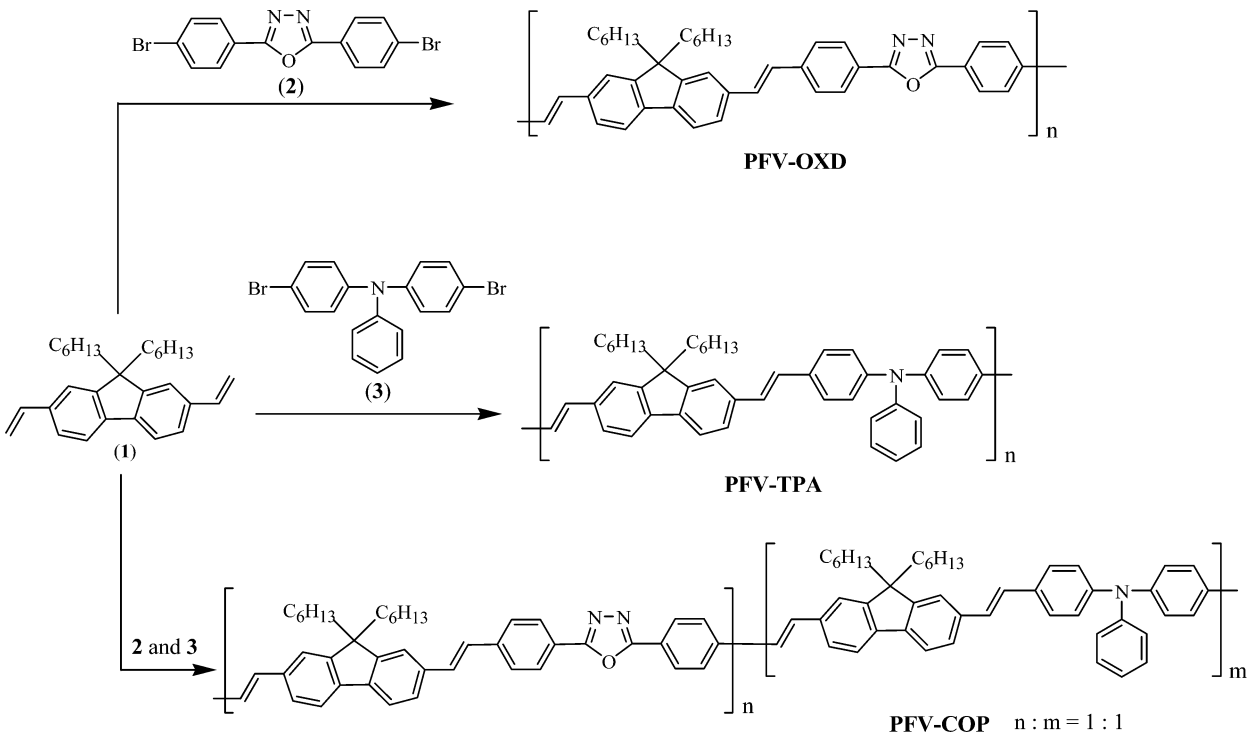

Cyclic voltammetry of the polymers was performed in acetonitrile with 0.1 M tetrabutylammonium hexafluorophosphate ($TBAPF_6$) as the supporting electrolyte at scan rates of 20−40 mV/s. Platinum wire electrodes were used as both counter and working electrodes, and silver/silver ion (Ag in 0.1 M $AgNO_3$ solution, from Bioanalytical Systems, Inc.) was used as a reference electrode. Using ferrocene as an internal standard, the potential values obtained were converted to versus SCE (saturated calomel electrode) and the corresponding ionization potential (IP) and electron affinity (EA) values were estimated from the onset redox potentials.

Fabrication and Characterization of LEDs. ITO-coated glass substrates (Delta Technologies Ltd., Stillwater, MN) were cleaned sequentially in ultrasonic baths of detergent solution, deionized water, chloroform, isopropanol, deionized water, and finally acetone. After drying the ITO substrates overnight at 60 °C in a vacuum, a 65 nm thick poly(ethylenedioxythiophene)/poly(styrene sulfonate) blend (PEDOT) hole injection layer was spin-coated on top of ITO and dried at 200 °C for 15 min under a vacuum. Before spin-coating, the as-received PEDOT solution was diluted by ∼25% with 1:1 (v/v) water/isopropanol and was then filtered through 0.45 μm PVDF syringe filters. Two types of OLEDs were fabricated with the copolymers as the emissive material, poly(*N*-vinylcarbazole) (PVK) as the hole-transport/electron-blocking layer and 1,3,5-tris-(*N*-phenylbenzimidizol-2-yl)benzene (TPBI) as the electron-transport/hole-blocking layer: type I: ITO/PEDOT/PVK/copolymer/TPBI/LiF/Al and type II: ITO/PEDOT/(PVK/copolymer blend)/TPBI/LiF/Al. For the type I devices, PVK was spin-coated from its 1.0 wt % solution in toluene to give a 35 nm thick film on PEDOT. The film was dried in a vacuum at 60 °C overnight. Thin films of the copolymers were obtained by spin-coating on top of PVK from ∼0.8 wt % solutions in chloroform and dried in a vacuum at 60 °C overnight. Before spin-coating, all the solutions were filtered through 0.2 μm PTFE syringe filters. The thickness of the copolymer films was measured by a Alpha-Step 500 Surface Profiler (KLA Tencor, Mountain View, CA). Because of the common solubility of PVK in chloroform, the interface between PVK and the copolymers is not flat; the total thickness of the composite PVK/copolymer bilayers was measured to be between 48 and 55 nm. For the type II devices, the binary blends of 95 wt % PVK and 5 wt % copolymers were made by mixing appropriate volumes of 0.75 wt % PVK solutions and 0.4 wt % copolymer solutions in chloroform. Films 35−40 nm thick of the blends were obtained on top of PEDOT by spin-coating.

In both sets of devices, 20 nm thick films of TPBI were obtained by evaporation from resistively heated quartz crucibles at a rate of ∼0.2 nm/s in a vacuum evaporator (Edwards Auto 306) at base pressures of $<9 \times 10^{-7}$ Torr. The chamber was vented with air to load the cathode materials, pumped back down, and then a 2-nm LiF and an ∼120 nm thick aluminum layer were sequentially deposited through a shadow mask without breaking vacuum to form active diode areas of 0.2 cm^2. To record the current−voltage data, we used an HP4155A semiconductor parameter analyzer (Yokogawa Hewlett-Packard, Tokyo), and the luminance was measured simultaneously with a model 370 optometer (UDT Instruments, Baltimore, MD) equipped with a calibrated sensor head (model 211) and a 5× objective lens. The device external quantum efficiencies were calculated using procedures reported previously.[3a,18b] All the device fabrication and characterization were done under ambient laboratory conditions

Results and Discussion

Synthesis and Characterization. The three new polyfluorenevinylene copolymers PFV−OXD, PFV−TPA, and PFV−COP that contain intrachain electron-accepting oxadiazole units, electron-donating triphenylamine units, and both donor and acceptor moieties, respectively, were synthesized by Heck coupling[32] according to Scheme 1. In particular, 9,9-dihexyl-2,7-divinylfluorene (**1**) reacted with 2,5-bis(4-bromophenyl)-1,3,4-oxadiazole (**2**) or bis(4-bromophenyl)phenylamine (**3**) in a molar ratio of 1:1 to afford the alternating copolymers PFV−OXD and PFV−TPA, respectively. **1** reacted with **2** and **3** in a molar ratio 2:1:1 to yield the statistical copolymer PFV−COP. These reactions took place in DMF utilizing triethylamine as an acid acceptor. Scheme 2 outlines the preparation of the dibromide derivative **2**. Specifically, 4-bromobenzonitrile reacted with a mixture of NH_4Cl and NaN_3 in DMF to afford 4-bromophenyltetrazole.[33] Finally, the latter reacted with 4-bromobenzoyl chloride in pyridine to afford **2**. The copolymers were purified by dissolving in THF and precipitating into methanol. The preparation yields were 48−57%. The number

Scheme 2

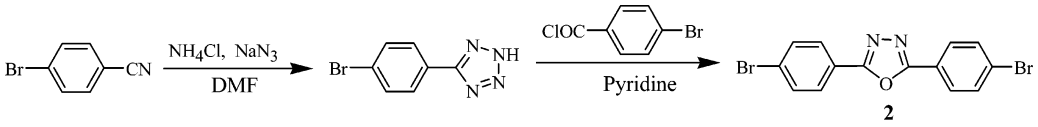

Table 1. Molecular Weights and Thermal Characteristics of Copolymers

copolymer	M_n[a]	M_w/M_n[a]	T_d[b] (°C)	T_g[c] (°C)
PFV−TPA	7 500	1.4	409	147
PFV−OXD	11 300	1.9	417	160
PFV−COP	9 800	1.6	411	154

[a] Molecular weights determined by GPC using polystyrene standards. [b] Decomposition temperature corresponding to 5% weight loss in N_2 determined by TGA. [c] Glass transition temperature determined by TMA.

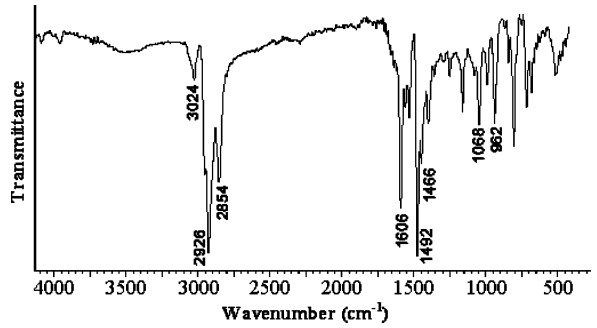

Figure 1. FT-IR spectrum of copolymer PFV−OXD.

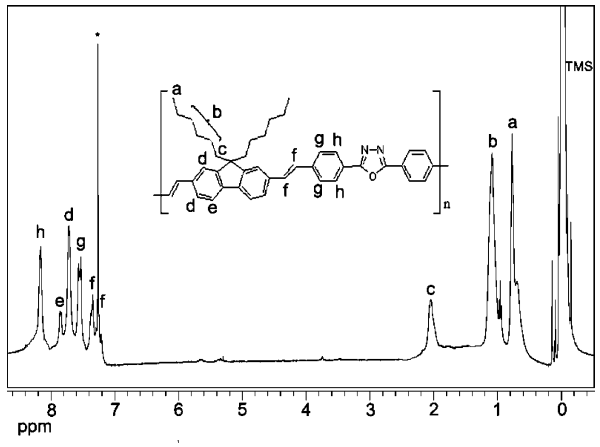

Figure 2. ^{1}H NMR spectrum of copolymer PFV−OXD in $CDCl_3$. The solvent peak is denoted by an asterisk.

average molecular weights (M_n) of the copolymers were 7500−11 300 with a polydispersity of 1.4−1.9 (Table 1). All the copolymers were soluble in common organic solvents such as THF, chloroform, chlorobenzene, and toluene.

The FT-IR and ^{1}H NMR spectra of the copolymers were consistent with their chemical structures. Figures 1 and 2 depict the IR and ^{1}H NMR spectra of PFV−OXD, respectively. The IR spectra of all copolymers had common absorption bands around 3024, 1606, 1492, 1466 (aromatic); 2926, 2854 (C−H stretching of the hexyl chains); and 962 cm^{-1} (trans olefinic bond). Besides these absorptions, PFV−OXD showed a band at 1068 cm^{-1} associated with the oxadiazole ring, while PFV−TPA showed bands at 1492, 1322, and 1278 cm^{-1} assigned to the C−N stretching of the triphenylamine moiety. The ^{1}H NMR spectrum of PFV−OXD (Figure 2) displayed a distinguishable multiplet at 8.16 ppm assigned to the four aromatic protons ortho to the electron deficient oxadiazole ring, while the resonances of the other aromatic protons were at 7.53−8.15 ppm. The olefinic protons appeared at 7.34−7.25 ppm. The resonances of these protons overlapped with those of the aromatic protons in the case of PFV−TPA and PFV−COP. Finally, the ^{1}H NMR spectra of all copolymers had peaks at ∼ 2.00, 1.00, and 0.75 ppm assigned to the aliphatic protons labeled "c", "b", and "a", respectively, of the hexyl groups (Figure 2). The ^{1}H NMR spectrum of PFV−OXD showed small but clear signals between 5 and 6 ppm from the protons CH_2═CH− of the vinyl end groups.

The thermal characteristics of the three copolymers were studied by TGA and TMA (Figure 3, Table 1). All three copolymers had high decomposition temperatures (T_d = 409−417 °C). The glass transition temperature (T_g) of the copolymers was determined by TMA using a loaded penetration probe (Table 1). It was obtained from the onset temperature of the baseline shift recorded during the second heating (inset of Figure 3). The T_g ranged from 147 to 160 °C and followed the trend PFV−OXD > PFV−COP > PFV−TPA. This suggests that incorporating 2,5-diphenyloxadiazole units along the copolymer backbones renders higher rigidity compared to the triphenylamine units. The T_g's of the current copolymers are slightly lower than that of poly(9,9-di-*n*-octylfluorene-2,7-vinylene) (T_g = 173 °C)[15] but higher than that of poly(fluorenevinylene-*co*-phenylenevinylene) (T_g = 110 °C).[16] Importantly, the T_g's of the current copolymers are significantly higher than that of poly(9,9-dialkylfluorene)s (T_g = 75−113 °C).[34] The relatively high T_g and T_d of the present copolymers bodes well for their OLED applications, since the lifetime of polymer LEDs is known to depend critically on the thermal stability of the active polymers.

Photophysical Properties. The normalized optical absorption and photoluminescence (PL) emission spectra of the three copolymers in dilute (10^{-5} M) toluene solution are shown in Figure 4, parts a and b. The absorption maxima are in the range of 406−422 nm corresponding to the $\pi-\pi^*$ transition of the polymer backbone. PFV−OXD has the most blue-shifted absorption maxima and highest-energy absorption onset at 460 nm among the three copolymers, suggesting increased disruption of π-conjugation caused by the oxadiazole linkage in the copolymer backbone. PFV−TPA had the most red-shifted absorption maximum at 422 nm and the lowest-energy absorp-

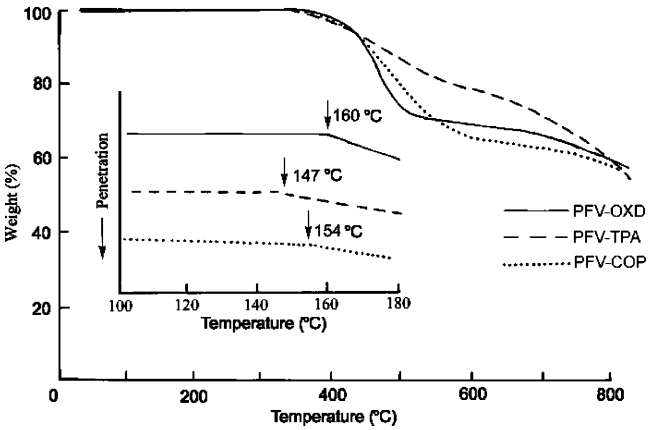

Figure 3. TGA thermograms of the three copolymers. The inset shows the TMA traces of the copolymers. Conditions: N_2 flow, 60 cm^3/min; heating rate, 20 °C/min for TGA and 10 °C/min for TMA.

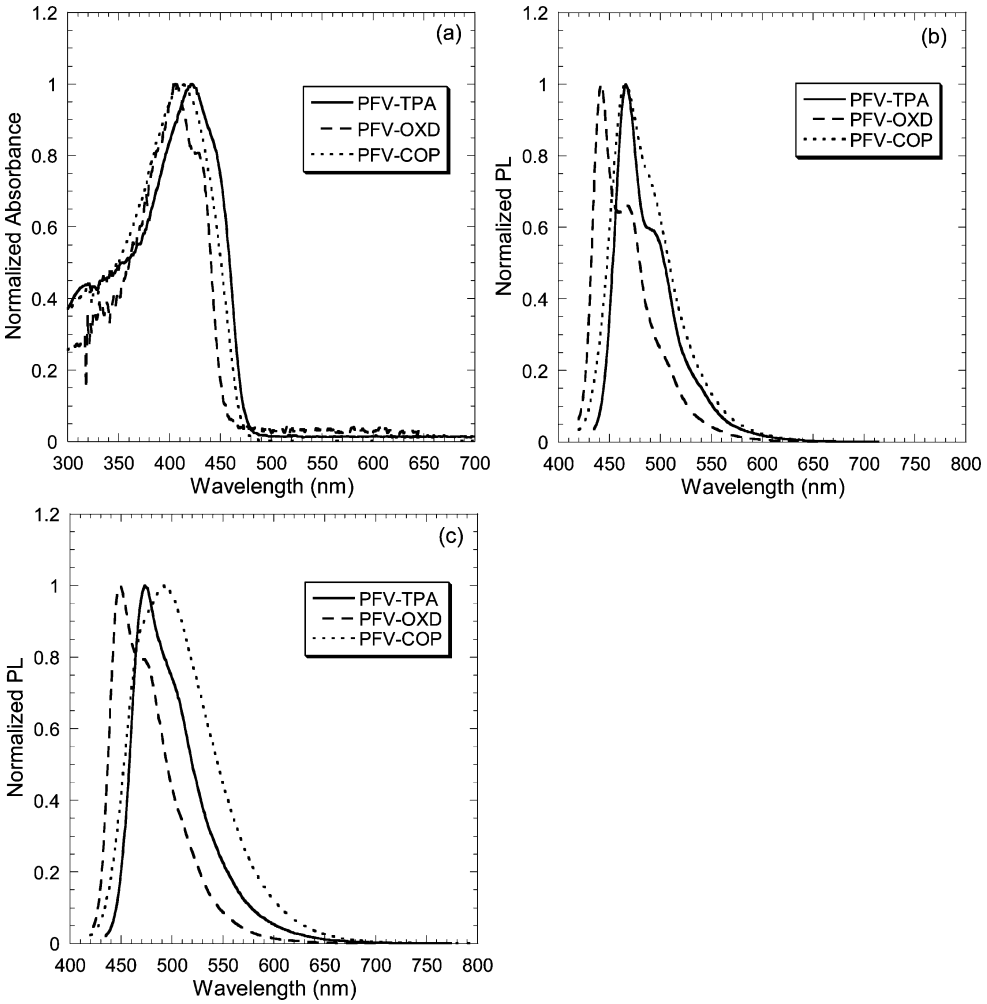

Figure 4. (a) Normalized optical absorption spectra of 10^{-5} M copolymer solutions in toluene. Normalized PL emission spectra of 10^{-5} M solutions of the copolymers in (b) toluene and(c) chloroform.

tion onset at 480 nm, indicating relatively longer conjugation lengths. PFV−COP containing both the oxadiazole and the triphenylamine units had an absorption maximum at 412 nm that lies between that of PFV−OXD and PFV−TPA. In the emission spectra, PFV−OXD had the most blue-shifted peak at 442 nm, like in absorption, while PFV−TPA and PFV−COP had identical emission maxima at 466 nm. The full width at half-maximum (fwhm) of the emission spectrum of PFV−COP (60 nm) is 10 nm larger than that of PFV−TPA (50 nm). These dilute solution emission spectra of PFV−TPA and PFV−COP are similar in terms of shape and peak position to that of poly-(9,9-dialkylfluorene-2,7-vinylene) (PFV).[13a]

Given that the current copolymers contain strong donor and acceptor units, unlike PFV, we wanted to investigate the presence of any intramolecular charge transfer (ICT) effects.[35] Thus, we also investigated the dilute solution photophysics of the three copolymers in chloroform, which has a higher dielectric constant ($\epsilon = 4.81$) compared to toluene ($\epsilon = 2.38$).[36] The optical absorption spectra of the copolymers in dilute (10^{-5} M) chloroform solutions (not shown) were almost identical to those in toluene solutions. Thus, the ground-state electronic structures of the copolymers are not much affected by the polarity of the solvent, suggesting a small dipole moment. Significant spectral shifts were observed in the emission spectra in chloroform (Figure 4c). The spectra of all three copolymers were broader and red-shifted in the higher-polarity solvent. The emission maxima of PFV−OXD, PFV−TPA, and PFV−COP were at 449, 473, and 492 nm, respectively. The fwhm of the emission spectra were 58, 62, and 92 nm, respectively. Thus, in the case of PFV−COP, the PL emission red-shifted by 26 nm and the fwhm increased by 32 nm in going from toluene to chloroform, clearly indicating the ICT character of the excited states. The extent of red-shift and spectral broadening was smaller in PFV−TPA and PFV−OXD, suggesting relatively weaker ICT effects.

Emission from charge-transfer excited states has been previously observed in fluorene copolymers containing strong electron donating and/or electron accepting groups.[19b,37] Increased excited-state ICT character generally leads to low PL quantum yield (ϕ_f) in emissive conjugated copolymers.[35,37] The estimated ϕ_f values of the current polymers in 10^{-5} M toluene solutions were 0.87, 0.76, and 0.81 for PFV−OXD, PFV−TPA, and PFV−COP, respectively. These ϕ_f values are quite high and similar compared to blue-emitting polyfluorenes. Thus, the strong ICT effects in the current PFV copolymers apparently do not quench their PL quantum yields as much, at least in solution. The photophysical properties of all the copolymers are summarized in Table 2.

Figure 5a shows the normalized optical absorption spectra of thin films of the three copolymers. They are similar to the absorption spectra in dilute solution, with absorption maxima of 411−424 nm, which are red-shifted by only 2−5 nm from the dilute solution. The similarity between the thin film and the dilute solution spectra suggests comparable ground state electronic structures of the copolymers, with not much aggregation in the solid state. Unlike the differences in the absorption onset observed in the solution spectra of the copolymers (Figure

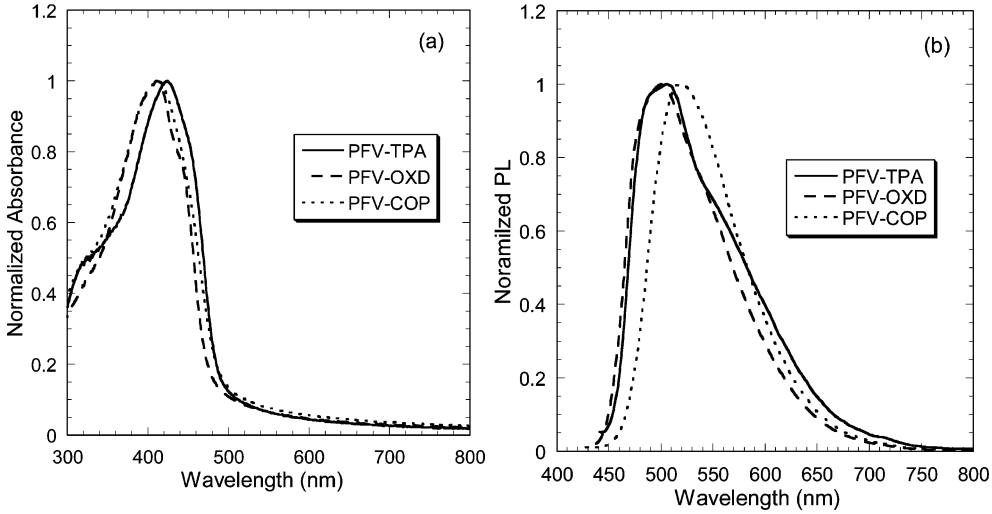

Figure 5. (a) Normalized optical absorption spectra and (b) normalized PL emission spectra of the copolymer thin films. Films were excited at their corresponding absorption maximum.

Table 2. Photophysical Properties of Copolymers

copolymer	$\lambda_{a,max}$[a] in solution (nm)	$\lambda_{f,max}$[b] in solution (nm)	Φ_f[c] in solution	$\lambda_{a,max}$[a] in thin film (nm)	$\lambda_{f,max}$[b] in thin film (nm)	E_g[d] (eV)
PFV−TPA	422	466	0.76	424	505	2.50
PFV−OXD	406	442	0.87	411	500	2.55
PFV−COP	412	466	0.81	411	520	2.50

[a] $\lambda_{a,max}$: The absorption maximum in toluene solution or in thin film. [b] $\lambda_{f,max}$: The PL emission maximum in toluene solution or in thin film. [c] Φ_f: PL quantum yield in 10^{-5} M toluene solution. [d] E_g: The optical band gap calculated from the onset of thin film absorption spectrum.

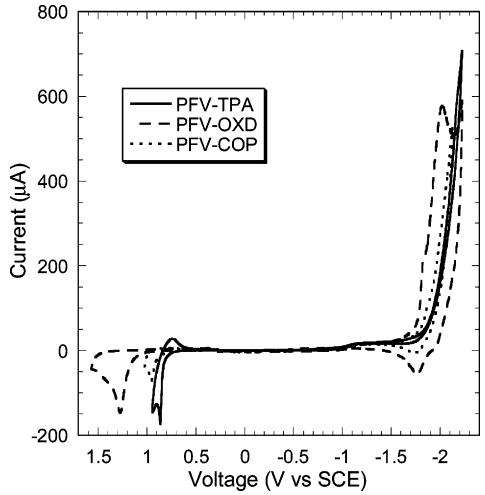

Figure 6. Cyclic voltammograms of copolymer thin films on Pt wires in 0.1 M $TBAPF_6$ in acetonitrile. The scan rates used were 20−40 mV/s.

4a), the absorption edges of the thin film spectra are all nearly identical. This suggests comparable conjugation lengths in the three copolymers in the solid state, leading to similar bulk electronic structures. The optical band gaps derived from the absorption edge of the thin film spectra gave similar values of 2.50−2.55 eV for all copolymers (Table 2). These band gaps are lower than that of poly(9,9-dihexylfluorene) (E_g = 2.9 eV)[4a] but similar to that of poly(9,9-dialkylfluorene-2,7-vinylene) (E_g = 2.6 eV).[15]

The normalized PL emission spectra of the copolymer thin films are shown in Figure 5b. Compared to the dilute solution emission spectra, the thin film spectra are red-shifted by 40−55 nm and are broader due to the inhomogeneous broadening effects in the solid state. PFV−TPA and PFV−OXD have closely spaced emission peaks at 505 and 500 nm, respectively, while PFV−COP has a peak at 520 nm. The steady increase in Stokes shift in the thin film from PFV−TPA (81 nm) to PFV−OXD (89 nm) to PFV−COP (109 nm) suggests greater ICT effects and correspondingly larger planarization of the copolymer backbone. Generally, the emission maxima of these copolymers are comparable to that of their corresponding trimer model compounds (471−510 nm)[17] and poly(9,9-dialkylfluorene-2,7-vinylene) (507 nm).[15]

Table 3. Redox Potentials and Electronic Structure Parameters of Copolymers

copolymer	E_{onset}[a] oxidation (V)	E_{onset}[a] reduction (V)	ionization potential IP (eV)[b]	electron affinity EA (eV)[c]	E_g^{el} (eV)[d]
PFV−TPA	0.80	−1.85	5.20	2.55	2.65
PFV−OXD	1.20	−1.75	5.60	2.65	2.95
PFV−COP	0.90	−1.80	5.30	2.60	2.70

[a] E_{onset} = onset potential versus SCE. [b] Determined from the onset oxidation potential. [c] Determined from the onset reduction potential. [d] Electrochemical band gap = IP − EA.

Electrochemical Properties. To understand the variation in the electronic structure of the PFV copolymers upon incorporation of donor triphenylamine and acceptor oxadiazole moieties, we performed cyclic voltammetry (CV) measurements on polymer films. The redox scans of all three copolymers are shown in Figure 6. PFV−TPA showed a quasi-reversible oxidation with an onset potential of +0.80 V vs SCE. PFV−COP had an irreversible oxidation with an onset potential of +0.90 V while PFV−OXD had the largest irreversible onset potential of +1.20 V. Taking −4.4 eV as the SCE energy level relative to vacuum, the ionization potential (IP) energy levels of PFV−TPA, PFV−COP, and PFV−OXD were estimated to be 5.20, 5.30, and 5.60 eV (Table 3). The presence of the oxadiazole moiety in PFV−OXD and PFV−COP renders their oxidation completely irreversible. However, in the reduction scans, the oxadiazole unit makes the reduction wave of PFV−OXD quasi-reversible while its absence in PFV−TPA renders its reduction wave completely irreversible and rather ill-defined. The onset reduction potential of PFV−OXD at −1.75 V is slightly higher than that of PFV−TPA and PFV−COP. This leads to an EA value of 2.65 eV for PFV−OXD, which is 0.1

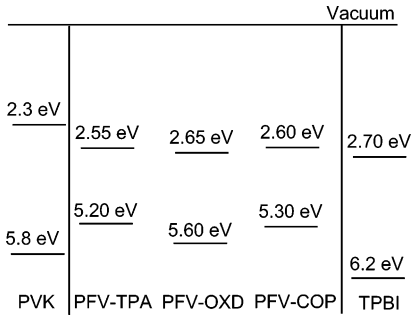

Figure 7. Energy levels (EA/IP) of the emissive copolymers (PFV−TPA, PFV−OXD, PFV−COP) and hole or electron-blocking materials (PVK, TPBI) used in the devices.

eV higher than that of PFV−TPA as would be expected with the presence of the electron-accepting oxadiazole moiety in the former. Overall, the EA values of all three copolymers are similar and comparable to those of poly(9,9-dialkylfluorene-2,7-vinylene)s (EA ∼ 2.6−2.7 eV),[13b,15a] suggesting insignificant changes in the LUMO energy manifold upon incorporation of donor triphenylamine and acceptor oxadiazole moieties. The presence of oxadiazole in PFV−OXD apparently leads to a 0.3 eV higher IP value compared to poly(9,9-dialkylfluorene-2,7-vinylene)s (IP ∼ 5.3 eV). All the electrochemical properties of the current copolymers are collected in Table 3. Although these PFV derivatives are D−A conjugated polymers, the observed electrochemical properties suggest that we do not realize true bipolar behavior in them, which has implications in relation to charge transport properties for their device applications.

Electroluminescent Properties. Single-layer light-emitting diodes (LEDs) of the type ITO/PEDOT/copolymer/LiF/Al were fabricated initially to investigate the electroluminescence (EL) properties of the PFV copolymers. However, poor performance was obtained from all copolymers with a maximum brightness of ∼70−190 cd/m^2. Importantly, the EL spectra observed from all three copolymers (not shown) were found to be highly voltage-dependent and were significantly red-shifted by up to 70 nm (in PFV−TPA) compared to their thin film PL emissions. We surmised that partial doping of the copolymers at the PEDOT/polymer interface could be responsible for the low brightness and the red-shifts in the EL spectra. Such charge transfer and doping processes have been observed at the interface of PEDOT and the emissive conjugated polymer in LEDs.[38] We thought that the addition of a buffer layer such as PVK between the PEDOT and the copolymer layer would help to minimize the doping problem and consequently stabilize the EL spectra. Hence, bilayer devices of the type ITO/PEDOT/PVK/copolymer/LiF/Al were fabricated and evaluated. The EL spectra (not shown) were indeed stabilized and did not change with applied voltage and had emission maxima that correlated well with the PL emissions of the PFV copolymers. However, the addition of the PVK layer did not improve the device performance at all. The brightness and efficiencies were similar to those obtained in the devices without the PVK layer. In an effort to enhance the performance of these copolymer LEDs, it was thought that an additional layer of electron-transport/hole-blocking material such as 1,3,5-tris(*N*-phenylbenzimidizol-2-yl)benzene (TPBI; IP = 6.2−6.7 eV, EA = 2.7 eV)[1e] would be useful, particularly given the low IPs of the current PFV copolymers. An energy level diagram showing all the HOMO/LUMO levels relevant to the LEDs is shown in Figure 7.

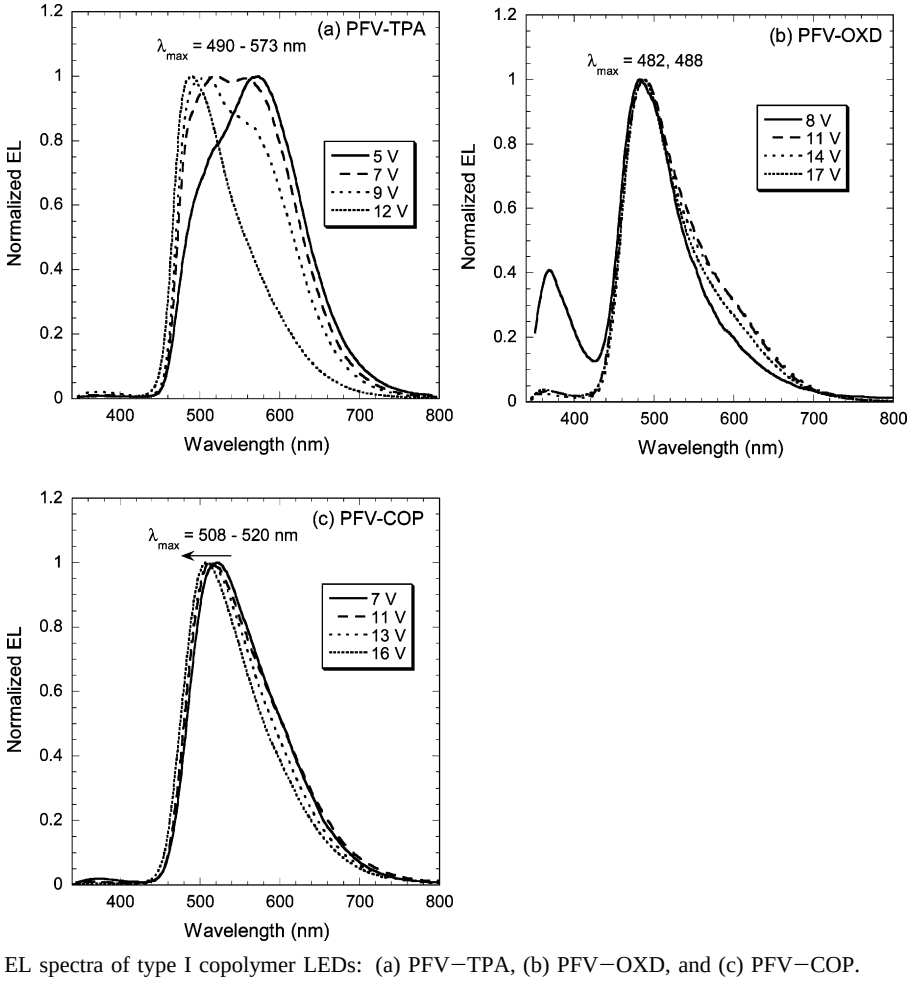

Figure 8. Normalized EL spectra of type I copolymer LEDs: (a) PFV−TPA, (b) PFV−OXD, and (c) PFV−COP.

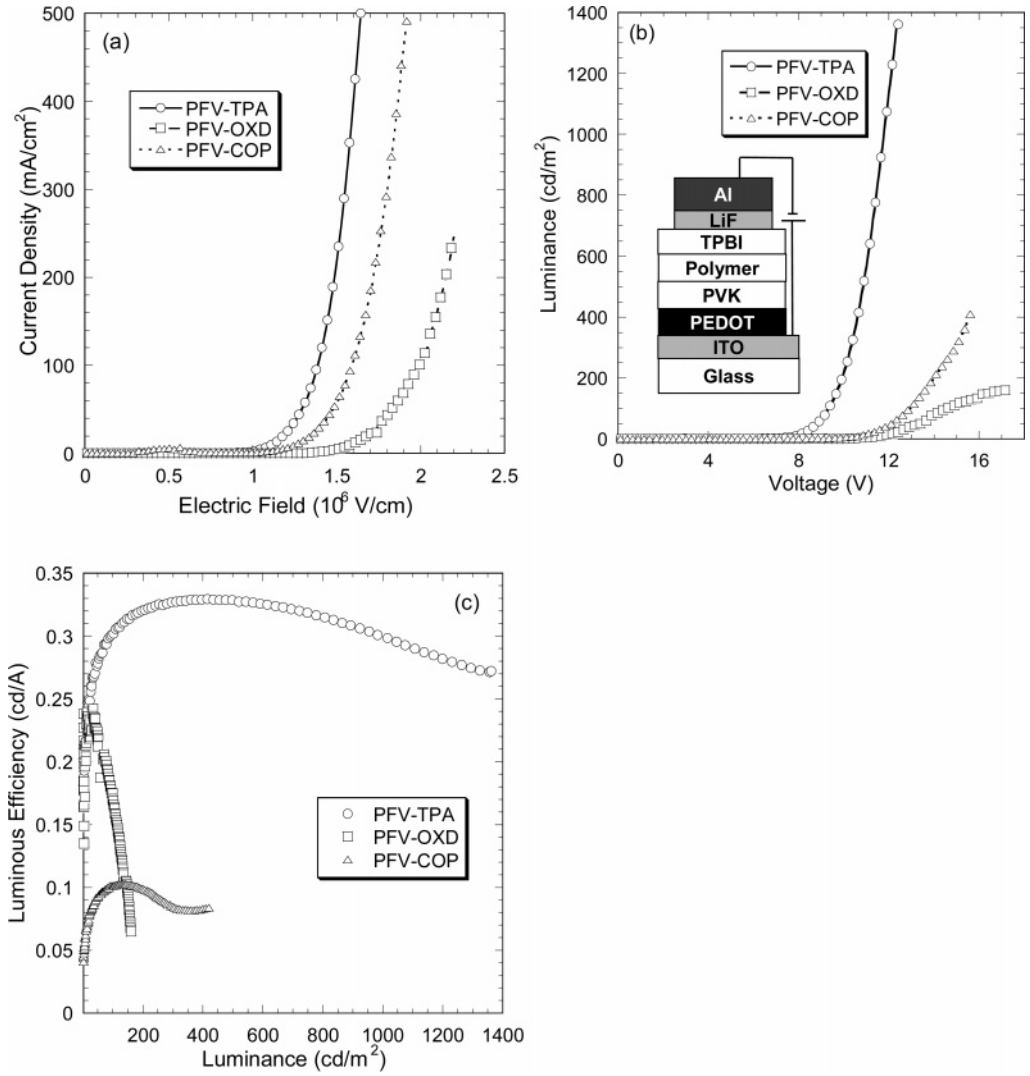

Figure 9. Type I copolymer LEDs: (a) current density−electric field and (b) luminance−voltage characteristics. Inset shows the device schematic. (c) Variation in luminous efficiency as a function of luminance of the diodes.

Figure 8, parts a−c, shows the normalized EL emission spectra of copolymer diodes of the type ITO/PEDOT/PVK/copolymer/TPBI/LiF/Al (type I). The EL emission of PFV−TPA (Figure 8a) significantly shifted with voltage from 573 nm at 5 V to 490 nm at 12 V. Such drastic changes in the EL spectra with voltage are highly undesirable in polymer LEDs. The 573 nm emission at the lowest voltage could likely be from an exciplex[39] at the PFV−TPA/TPBI interface given the favorable energy levels (Figure 7). Such dramatic shifts in the EL spectra were not observed in diodes with PFV−OXD and PFV−COP, as shown in parts b and c of Figure 8, respectively. Clearly, exciplex-type interactions are not expected at the PFV−COP/TPBI or PFV−OXD/TPBI interface by virtue of the fact that the copolymers contain acceptor moieties. PFV−OXD had stable EL emission with a maximum at 482−488 nm, which is blue-shifted by 12−18 nm from its thin film PL emission maximum. The peak in the UV region at ∼370 nm is from the TPBI layer, which seems to dominate only at low voltages. At the maximum voltage, the PFV−OXD diode emits a light green color with CIE coordinates of (0.25, 0.38). The EL spectra of the PFV−COP diode (Figure 8c) have maxima at 508−520 nm that slightly blue shift with increasing voltage, which match well with its thin-film PL emission. At the maximum voltage (16 V), the diode emits yellowish-green color with CIE coordinates of (0.31, 0.51).

The current density−electric field and luminance−voltage characteristics of the type I copolymer diodes are shown in Figure 9, parts a and b, respectively. Both PFV−TPA and PFV−COP diodes have similar turn-on electric fields of ∼ 1 MV/cm, while the PFV−OXD diode has a higher turn-on at ∼1.5 MV/cm. This can be understood to arise from the 0.3 eV higher IP value of PFV−OXD compared to both PFV−TPA and PFV−COP, which makes hole injection into the emissive PFV−OXD copolymer more difficult. At the same electric fields, the currents passing through the PFV−OXD diode are much lower than the other two copolymers which contain the donor triphenylamine groups and thus are expected to have better hole transport properties. The variation in the brightness of the LEDs as a function of applied voltage is shown in Figure 9b. The maximum luminance was 1360, 160, and 420 cd/m^2 for the PFV−TPA, PFV−OXD, and PFV−COP diodes, respectively. The corresponding maximum luminous efficiencies were 0.33, 0.17, and 0.10 cd/A. The addition of the TPBI layer benefited the PFV−TPA diode the most, with a 10× higher brightness compared to previous diodes without the TPBI layer. This suggests that holes are the majority carriers in the PFV−TPA diode due to the presence of the strong donor triphenylamine groups. PFV−OXD had the lowest performance among the three copolymers likely due to its higher IP and lower thin-film PL quantum yield due to the stronger ICT effects. The type I device characteristics

Table 4. Device Characteristics of Type I LEDs: ITO/PEDOT/PVK/Copolymer/TPBI/LiF/Al[a]

copolymer	drive voltage V (V)	current density J (mA/cm^2)	luminance L (cd/m^2)	luminous efficiency (cd/A)	EQE[b] (%)	CIE (x, y)
PFV−TPA	12.4	500	1360	0.27	0.11	(0.26, 0.45)
	10.5	*109*	*360*	*0.33*	*0.12*	*(0.35, 0.49)*
PFV−OXD	17.2	246	160	0.07	0.03	(0.25, 0.39)
	14.5	*60*	*101*	*0.17*	*0.07*	*(0.27, 0.40)*
PFV−COP	15.6	500	419	0.08	0.03	(0.31, 0.51)
	13.4	*138*	*142*	*0.10*	*0.04*	*(0.33, 0.52)*

[a] The values in italic correspond to the maximum efficiency at a brightness ≥100 cd/m^2. [b] External quantum efficiency.

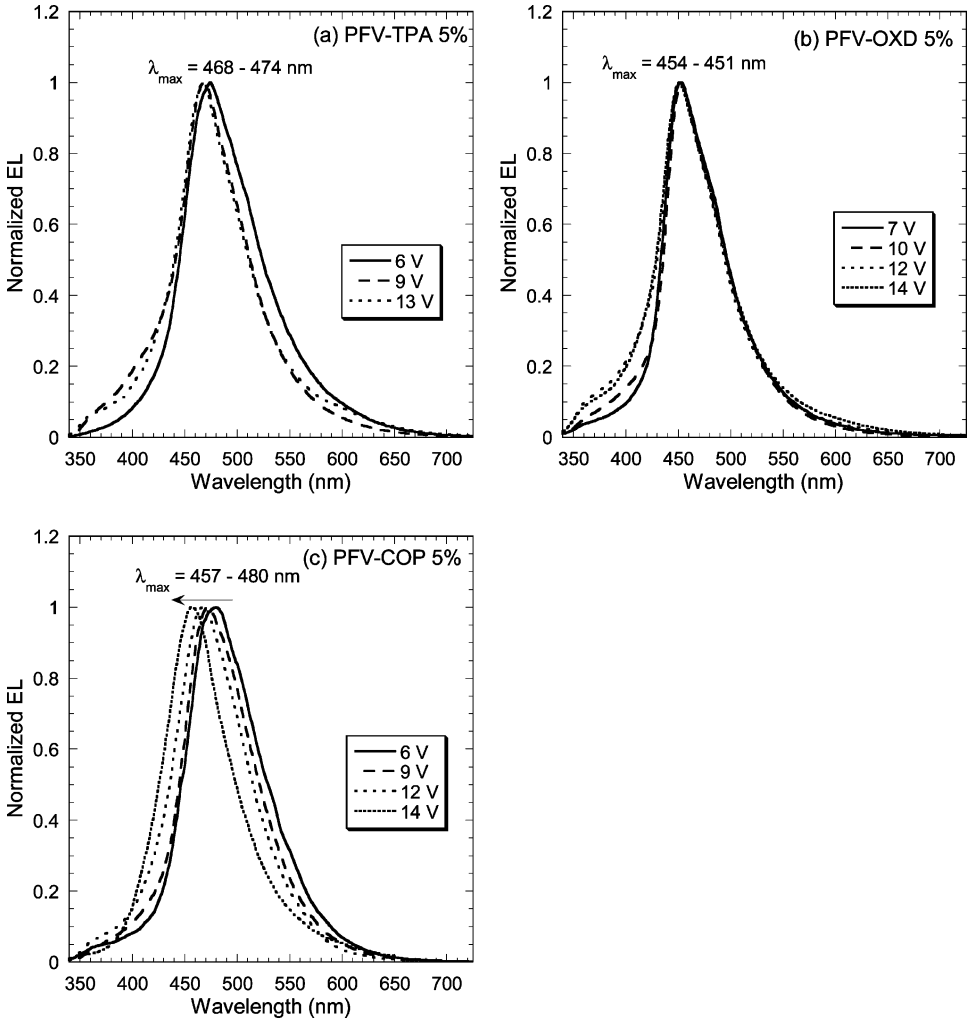

Figure 10. Normalized EL spectra of type II copolymer LEDs based on 5 wt % blends of the copolymers with PVK: (a) PFV−TPA, (b) PFV−OXD, and (c) PFV−COP.

of the three copolymers are summarized in Table 4. Figure 9c shows the variation in the luminous efficiency of the type I devices versus luminance for all the copolymers. It is clear that PFV−TPA gives the superior device performance among the three copolymers. The maximum efficiency is 0.33 cd/A at a brightness of 360 cd/m^2 and it decreases slightly to 0.27 cd/A at the maximum brightness of 1360 cd/m^2. PFV−OXD had higher efficiencies than PFV−COP at brightnesses lower than 150 cd/m^2, but at the higher luminances, PFV−COP gave the better performance. These results demonstrate the significance of the choice of the D and A moieties to attain the optimum balance between hole and electron injection/transport and the desired high EL efficiency in emissive copolymers.

To try to further improve the performance of the copolymer diodes, we fabricated devices of the type ITO/PEDOT/(PVK/copolymer)/TPBI/LiF/Al (type II) wherein the copolymers were blended with PVK at ratios of 5:95 w/w. The rationale behind blending the copolymers at such dilute fractions into the PVK matrix was to achieve enhanced performance by exploiting any possible energy transfer effects. The normalized EL emission spectra of the type II copolymer diodes are shown in Figure 10, parts a−c. The dramatic voltage dependence that was seen in the type I PFV−TPA diodes (Figure 8a) was completely absent in the corresponding type II diodes. The type II PFV−TPA devices (Figure 10a) had stable EL emission with maxima in the 468−474 nm range, that are blue-shifted by ∼35 nm compared to the PL emission of a neat thin film of PFV−TPA. This blue-shift in the blend diodes can be completely understood to arise from the dilution effects to be expected in the 5 wt % binary blends with PVK. Infact, the PL emission maximum of the PVK/PFV−TPA (95:5) blend film was found to be at 470 nm (not shown), which matches very well with the observed

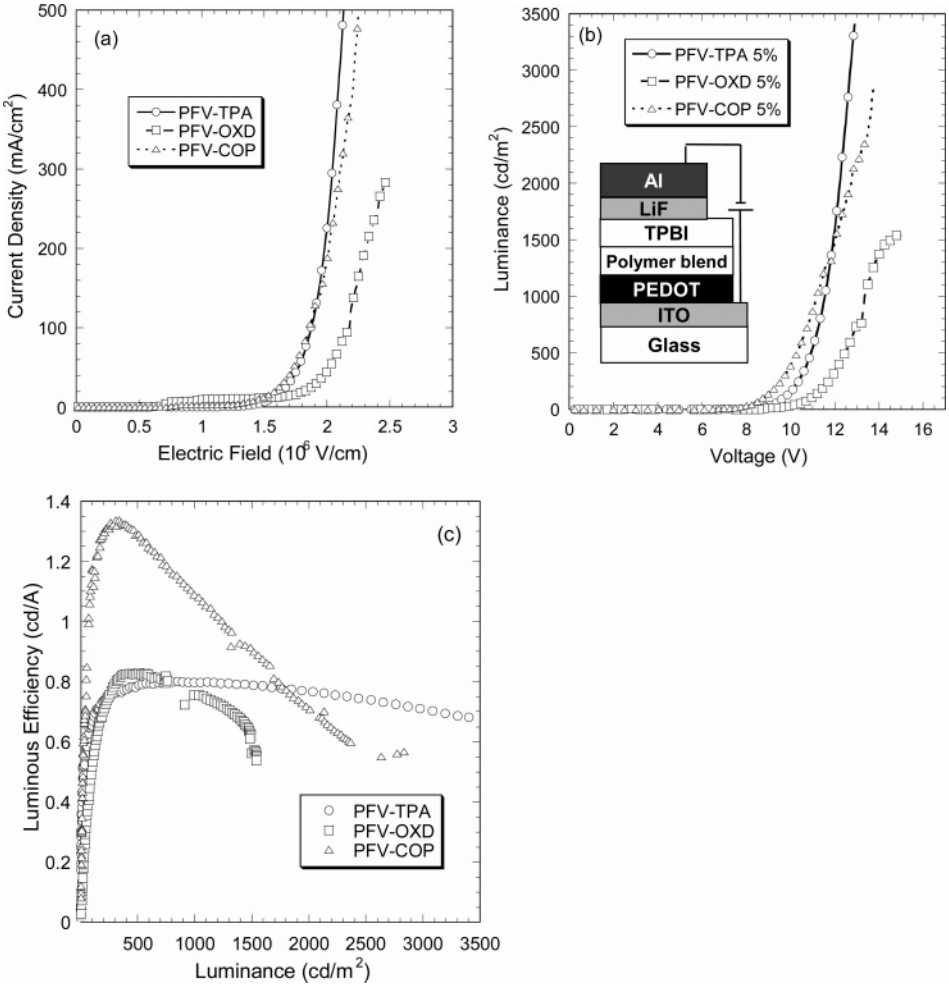

Figure 11. Type II copolymer LEDs: (a) current density−electric field and (b) luminance−voltage characteristics. Inset shows the device schematic. (c) Variation in luminous efficiency as a function of luminance of the diodes.

Table 5. Device Characteristics of Type II LEDs: ITO/PEDOT/(PVK/Copolymer)/ TPBI/LiF/Al[a]

copolymer	drive voltage V (V)	current density J (mA/cm^2)	luminance L (cd/m^2)	luminous efficiency (cd/A)	EQE[b] (%)	CIE (x, y)
PFV−TPA	12.9	500	3400	0.68	0.49	(0.18, 0.22)
	11.4	*106*	*850*	*0.80*	*0.63*	*(0.17, 0.20)*
PFV−OXD	14.9	280	1540	0.55	0.52	(0.17, 0.16)
	12.5	*62*	*510*	*0.83*	*0.83*	*(0.16, 0.15)*
PFV−COP	13.7	500	2830	0.57	0.51	(0.17, 0.16)
	9.8	*25*	*338*	*1.34*	*0.89*	*(0.17, 0.24)*

[a] All blends contain 95 wt % PVK and 5 wt % of PFV copolymers. The values in italic correspond to the maximum efficiency at a brightness ≥100 cd/m^2. [b] External quantum efficiency.

EL spectra. As a result of the blue-shift, the EL emission colors from the PFV−TPA blend diode are blue (CIE = 0.18, 0.22) instead of the light-green colors seen in its type I diode. Similar blue-shifts were observed in the EL spectra of the blends of PFV−OXD (Figure 10b) and PFV−COP (Figure 10c) compared to their corresponding neat film diodes. PFV−OXD blends had EL emission maxima at ∼450 nm that did not change with applied voltage, leading to stable blue EL (CIE = 0.16, 0.15). In the case of the PFV−COP blends (Figure 10c), the EL emission spectra blue-shifted with increasing voltage from 480 nm at 6 V to 457 nm at 14 V. For comparison, the PL emission maximum of the PVK/PFV−COP (95:5) blend film was found to be at 483 nm (not shown). The EL colors were in the blue region of the CIE plot with coordinates of (0.17, 0.24) at 10 V and (0.17, 0.16) at 16 V. We note that although the emission band of the host PVK used in all of these blends is centered at around 420 nm,[40] it is rather weak and the energy levels of PVK favor efficient energy transfer to the copolymers whose EL bands are in the 450−483 nm range. Thus, by blending into PVK at dilute fractions, the EL colors of the current copolymers were tuned from yellow-green to blue due to the chromophore dilution.

The current density−electric field and luminance−voltage characteristics of the type II copolymer diodes are shown in Figure 11, parts a and b, respectively. Similar to the type I diodes, the type II PFV−TPA and PFV−COP diodes had lower turn-on electric fields (∼1.4 MV/cm) compared to that of the PFV−OXD diode (∼1.8 MV/cm). Also, the currents passing through the PFV−OXD blend diode are much lower than those in the other two copolymer diodes at the same electric fields. Figure 11b shows the variation in the luminance of the blend LEDs as a function of applied voltage. The maximum luminance was found to be 3400, 1770, and 2830 cd/m^2 for the PFV−TPA, PFV−OXD, and PFV−COP blend diodes, respectively.

The corresponding maximum luminous efficiencies were 0.80, 0.83, and 1.34 cd/A. Thus, factors of 3−11 enhancements in the brightness and 5−10 in the efficiencies were achieved in going from the neat copolymer thin films to their dilute blends. These dramatic improvements in the copolymer device performance are thought to arise from the increased relative PL emission yields in the blends compared to their neat thin films. All the type II device characteristics of the three copolymers are summarized in Table 5. Figure 11c shows the variation in the luminous efficiency of the type II diodes with luminance for all the copolymer blends. Here, copolymer PFV−COP gives the most superior performance among the three copolymers. The maximum efficiency is 1.34 cd/A (at 338 cd/m^2) and it decreases to 0.57 cd/A at the maximum brightness of 2830 cd/m^2. PFV−TPA and PFV−OXD blends seem to have similar efficiencies till luminances of up to 1000 cd/m^2, beyond which the PFV−OXD blends give relatively lower efficiencies. The luminous efficiency of PFV−TPA diodes, both type I and type II, remain fairly constant over the entire brightness range of the diodes, suggesting balanced charge injection and recombination at all electric fields. Thus, blending the PFV copolymers into PVK turned out to be an attractive option since stable blue EL with relatively high performance was achieved from the corresponding blend diodes.

Conclusions

We have synthesized new polyfluorenevinylene copolymers containing triphenylamine electron donor and/or bis(phenyl)-oxadiazole electron acceptor moieties along the backbone and used the materials to achieve efficient electroluminescence with colors ranging from blue to greenish-yellow. The copolymers had high glass transition temperatures of 147−160 °C. The HOMO/LUMO energy levels of the copolymers were tuned by addition of the donor and acceptor segments onto the polyfluorenevinylene backbone. The copolymers emitted blue-green colors in dilute solution with high PL quantum yields of 0.76−0.87. The presence of the donor/acceptor moieties in the copolymers led to intramolecular charge-transfer excited states. Greenish-yellow electroluminescence was achieved from diodes based on neat copolymer thin films with luminances of 160−1360 cd/m^2 that varied with the copolymer composition. Stable blue EL (CIE = 0.17, 0.16) was obtained in diodes based on dilute binary blends of the copolymers with poly(vinyl carbazole) giving luminances of 1770−3400 cd/m^2 and luminous efficiencies of up to 1.34 cd/A. These results demonstrate that the electron-donating strength of the donor moiety and the electron-accepting strength of the acceptor moiety are critical design parameters that affect the EL efficiency of emissive donor−acceptor copolymers.

Acknowledgment. Work at the University of Washington was supported by the NSF (Grant CTS-0437912), the Air Force Office of Scientific Research (Grant F49620-03-1-0162), and the NSF STC MDITR (Grant DMR-0120967).

References and Notes

(1) Reviews: (a) Bernius, M. T.; Inbasekaran, M.; O'Brien, J.; Wu, W. *Adv. Mater.* **2000**, *12*, 1737. (b) Kraft, A.; Grimsdale, A. C.; Holmes, A. B. *Angew. Chem., Int. Ed.* **1998**, *37*, 402. (c) Millard, I. S. *Synth. Met.* **2000**, *111*−*112*, 119. (d) Wu, W.; Inbasekaran, M.; Hudack, M.; Welsh, D.; Yu, W.; Cheng, Y.; Wang, C.; Kram, S.; Tacey, M.; Bernius, M.; Fletcher, R.; Kiszka, K.; Munger, S.; O'Brien, J. *Microelectronics J.* **2004**, *35*, 343. (e) Kulkarni, A. P.; Tonzola, C. J.; Babel, A.; Jenekhe, S. A. *Chem. Mater.* **2004**, *16*, 4556. (f) Mitschke, U.; Bäurele, P. *J. Mater. Chem.* **2000**, *10*, 1471. (g) Akcelrud, L. *Prog. Polym. Sci.* **2003**, *28*, 875.

(2) Braun, D.; Heeger, A. J. *Appl. Phys. Lett.* **1991**, *58*, 1982.

(3) (a) Kulkarni, A. P.; Jenekhe, S. A. *Macromolecules* **2003**, *36*, 5285. (b) Weinfurtner, K-H.; Fujikawa, H.; Tokito, S.; Taga, Y. *Appl. Phys. Lett.* **2000**, *76*, 250. (c) Grice, A. W.; Bradley, D. D. C.; Bernius, M. T.; Inbasekaran, M.; Wu, W. W.; Woo, E. P. *Appl. Phys. Lett.* **1998**, *73*, 629.

(4) (a) Neher, D. *Macromol. Rapid Commun.* **2001**, *22*, 1365. (b) Scherf, U.; List, E. J. W. *Adv. Mater.* **2002**, *14*, 477. (c) Bliznyuk, V. N.; Carter, S. A.; Scott, J. C.; Klärner, G.; Miller, R. D.; Miller, D. C. *Macromolecules* **1999**, *32*, 361.

(5) (a) List, E. J. W.; Guentner, R.; Scanducci de Freitas, P.; Scherf, U. *Adv. Mater.* **2002**, *14*, 374. (b) Panozzo, S.; Vial, J-C.; Kervella, Y.; Stéphan, O. *J. Appl. Phys.* **2002**, *92*, 3495. (c) Gong, X.; Iyer, P. K.; Moses, D.; Bazan, G. C.; Heeger, A. J.; Xiao, S. S. *Adv. Funct. Mater.* **2003**, *13*, 325. (d) Kulkarni, A. P.; Kong, X.; Jenekhe, S. A. *J. Phys. Chem. B* **2004**, *108*, 8689.

(6) (a) Janietz, S.; Bradley, D. D. C.; Grell, M.; Giebeler, C.; Inbasekaran, M.; Woo, E. P. *Appl. Phys. Lett.* **1998**, *73*, 2453. (b) Babel, A.; Jenekhe, S. A. *Macromolecules* **2003**, *36*, 7759.

(7) Brown, T. M.; Kim, J. S.; Friend, R. H.; Cacialli, F.; Daik, R.; Feast, W. J. *Appl. Phys. Lett.* **1999**, *75*, 1679.

(8) Ego, C.; Grimsdale, A. C.; Uckert, F.; Yu, G.; Srdanov, G.; Müllen, K. *Adv. Mater.* **2002**, *14*, 809.

(9) Sainova, D.; Miteva, T.; Nothofer, H. G.; Scherf, U.; Glowacki, I.; Ulanski, J.; Fujikawa, H.; Neher, D. *Appl. Phys. Lett.* **2000**, *76*, 1810.

(10) Bernius, M.; Inbasekaran, M.; Woo, E.; Wu, W.; Wujkowski, L. *J. Mater. Sci.: Mater. Electron.* **2000**, *11*, 111.

(11) Palilis, L. C.; Lidzey, D. G.; Redecker, M.; Bradley, D. D. C.; Inbasekaran, M.; Woo, E. P.; Wu, W. W. *Synth. Met.* **2000**, *111*, 159.

(12) Nomura, K.; Moromoto, H.; Imanishi, Y.; Ramhani, Z.; Geerts, Y. *J Polym. Sci., Part A: Polym. Chem.* **2001**, *39*, 2463.

(13) (a) Cho, H. N.; Kim, D. Y.; Kim, J. K.; Kim, C. Y. *Synth. Met.* **1997**, *91*, 293. (b) Mikroyannidis, J. A.; Yu, Y.-J.; Lee, S.-H.; Jin, J.-I. *J. Polym. Sci., Part A: Polym. Chem.* **2006**, *44*, 4494. (c) Barberis, V. P.; Mikroyannidis, J. A.; Cimrova, V. *J. Polym. Sci., Part A: Polym. Chem.* **2006**, *44*, 5750.

(14) Ahn, T.; Shim, H.-K. *Synth. Met.* **2001**, *121*, 1663.

(15) (a) Jin, S.-H.; Park, H.-J.; Kim, J. Y.; Lee, K.; Lee, S.-P.; Moon, D.-K.; Lee, H.-J.; Gal, Y.-S. *Macromolecules* **2002**, *35*, 7532. (b) Jin, Y.; Ju, J.; Kim, J.; Lee, S.; Kim, J. Y.; Park, S. H.; Son, S.-M.; Jin, S.-H.; Lee, K.; Suh, H. *Macromolecules* **2003**, *36*, 6970.

(16) Lopez, L. C.; Strohriegl, P.; Stübinger, T. *Macromol. Chem. Phys.* **2002**, *203*, 1926.

(17) Mikroyannidis, J. A.; Fenenko, L.; Adachi, C. *J. Phys. Chem. B* **2006**, *110*, 20317.

(18) (a) Shu, C.-F.; Dodda, R.; Wu, F.-I.; Liu, M. S.; Jen, A. K.-Y. *Macromolecules* **2003**, *36*, 6698. (b) Kulkarni, A. P.; Zhu, Y.; Jenekhe, S. A. *Macromolecules* **2005**, *38*, 1553. (c) Kulkarni, A. P.; Kong, X. X.; Jenekhe, S. A. *Macromolecules* **2006**, *39*, 8699.

(19) (a) Peng, Z. H.; Bao, Z. N.; Galvin, M. E. *Chem. Mater.* **1998**, *10*, 2086. (b) Zhu, Y.; Gibbons, K. M.; Kulkarni, A. P.; Jenekhe, S. A. *Macromolecules* **2007**, *40*, 804.

(20) (a) Barberis, V. P.; Mikroyannidis, J. A. *J. Polym. Sci., Part A: Polym. Chem.* **2006**, *44*, 3556. (b) Karastatiris, P.; Mikroyannidis, J. A.; Spiliopoulos, I. K.; Kulkarni, A. P.; Jenekhe, S. A. *Macromolecules* **2004**, *37*, 7867. (c) Mikroyannidis, J. A.; Spiliopoulos, I. K.; Kasimis, T. S.; Kulkarni, A. P.; Jenekhe, S. A. *Macromolecules* **2003**, *36*, 9295.

(21) Adachi, C.; Tsutsui, T.; Saito, S. *Appl. Phys. Lett.* **1989**, *55*, 1489.

(22) Schultz, B.; Bruma, M.; Brehmer, L. *Adv. Mater.* **1997**, *9*, 601.

(23) (a) Thelakkat, M.; Schmidt, H.-W. *Polym. Adv. Technol.* **1998**, *9*, 429. (b) Wang, C.; Jung, G.-Y.; Batsanov, A. S.; Bryce, M. R.; Petty, M. C. *J. Mater. Chem.* **2002**, *12*, 173.

(24) (a) Bellmann, S. E.; Shaheen, R. H.; Grubbs, S. R.; Marder, B. K.; Peyghambarian, N. *Chem. Mater.* **1999**, *11*, 399. (b) Hancock, J. M.; Gifford, A. P.; Zhu, Y.; Lou, Y.; Jenekhe, S. A. *Chem. Mater.* **2006**, *18*, 4924.

(25) (a) Sonar, P.; Zhang, J.; Grimsdale, A. C.; Mullen, K.; Surin, M.; Lazzzaroni, R.; Leclere, P.; Tierney, S.; Heeney, M.; McCulloch, I. *Macromolecules* **2004**, *37*, 709. (b) Huang, B.; Li, J.; Chen, L.; Qin, J.; Di, C.; Yu, G.; Liu, Y. *J. Polym. Sci., Part A: Polym. Chem.* **2005**, *43*, 4517. (c) Sung, H.-H.; Lin, H.-C. *J. Polym. Sci., Part A: Polym. Chem.* **2005**, *43*, 2700.

(26) Yang, J.; Jiang, C.; Zhang, Y.; Yang, R.; Yang, W.; Hou, Q.; Cao, Y. *Macromolecules* **2004**, *37*, 1211.

(27) Lee, J. K.; Klaerner, G.; Miller, R. D. *Chem. Mater.* **1997**, *11*, 1083.

(28) McKean, D. R.; Parrinello, G.; Renaldo, A. F.; Stille, J. K. *J. Org. Chem.* **1987**, *52*, 422.

(29) Shin, D.-C.; Ahn, J.-H.; Kim, Y.-H.; Kwon, S.-K. *J. Polym. Sci., Part A: Polym. Chem.* **2000**, *38*, 3086.

(30) Kim, S. W.; Shim, S. C.; Kim, D. Y.; Kim, C. Y. *Synth. Met.* **2001**, *122*, 363.

(31) Heinrich, G.; Schoof, S.; Gusten, H. *J. Photochem.* **1974**, *3*, 315.
(32) Ziegler, C. B., Jr.; Heck, R. F. *Org. Chem.* **1978**, *43*, 2941.
(33) Hou, S.; Chan, W. K. *Macromolecules* **2002**, *35*, 850.
(34) Grell, M.; Bradley, D. D. C.; Inbasekaran, M.; Woo, E. P. *Adv. Mater.* **1997**, *9*, 798.
(35) Jenekhe, S. A.; Lu, L.; Alam, M. M. *Macromolecules* **2001**, *34*, 7315.
(36) Reichardt, C. *Solvents and Solvent Effects in Organic Chemistry*; Verlag Chemie: New York, 1988.
(37) (a) Wu, W.-C.; Liu, C.-L.; Chen, W.-C. *Polymer* **2006**, *47*, 527. (b) Redecker, M.; Bradley, D. D. C.; Baldwin, K. J.; Smith, D. A.; Inbasekaran, M.; Wu, W. W.; Woo, E. P. *J. Mater. Chem.* **1999**, *9*, 2151.
(38) Peisert, H.; Knupfer, M.; Zhang, F.; Petr, A.; Dunsch, L.; Fink, J. *Appl. Phys. Lett.* **2003**, *83*, 3930.
(39) (a) Jenekhe, S. A.; Osaheni, J. A. *Science* **1994**, *265*, 765. (b) Osaheni, J. A.; Jenekhe, S. A. *Macromolecules* **1994**, *27*, 739.
(40) Hu, B.; Yang, Z.; Karasz, F. E. *J. Appl. Phys.* **1994**, *76*, 2419.

MA071504L